

BEAM BY DESIGN: CURRENT PULSE SHAPING THROUGH LONGITUDINAL DISPERSION CONTROL

T. K. Charles*, D. M. Paganin, School of Physics and Astronomy, Monash University, Australia
 M. J. Boland¹, R. T. Dowd, Australian Synchrotron, Clayton, Australia
¹also at School of Physics, University of Melbourne, 3010, Victoria, Australia

Abstract

Electron beams traversing a dispersive region, such as a bunch compressor and some transport line can form caustic lines and surfaces corresponding to regions of maximum electron density, which influence the current pulse shape. In this paper, we present a technique to manipulate the longitudinal phase space distribution to achieve an arbitrary, desired current pulse shape. We show how sextupole magnets (and in certain circumstances, octupole magnets), placed within a dispersive region can be used to generate the conditions required for a flexible technique of current pulse shaping that avoids truncation through collimation.

INTRODUCTION

Many applications that require current profile shaping have been proposed by the accelerator physics community. These include: creating linearly ramped current profiles for optimal plasma acceleration [1, 2], current profiles shaped for suppression of coherent synchrotron radiation induced emittance growth [3], removal of current spikes for improved FEL performance [4–6] and optimal current profiles for free electron laser applications [7], to name just a few.

In this paper, we illustrate how longitudinal phase space manipulation can be used to obtain arbitrarily-shaped current profiles. This is an alternative to the techniques requiring collimation or laser beam interference.

CURRENT PULSE SHAPE

The parametric form for the local compression ratio (z , C_l), parameterized by z_i – the initial longitudinal position of an electron with respect to the center of the bunch - for a bunch through a dispersive region was derived in reference [8] to be,

$$z(z_i) = z_i + R_{56}\delta(z_i) + T_{566}\delta^2(z_i) + U_{5666}\delta^3(z_i) \quad (1a)$$

$$C_l(z_i) = \frac{\rho(z_i)}{1 + \delta'(z_i)[R_{56} + 2T_{566}\delta(z_i) + 3U_{5666}\delta^2(z_i)]} \quad (1b)$$

where $\delta(z_i)$ is the shape of the initial longitudinal phase space distribution or chirp (often described by a high-order polynomial), a dash denotes a derivative with respect to z_i , $\rho(z_i)$ is the initial charge-density distribution (often considered Gaussian or super Gaussian) and R_{56} , T_{566} , and U_{5666}

are the first-, second-, and third-order longitudinal dispersion values respectively.

Whilst Eq. (1) describes the local compression ratio, the current profile should display the same shape and can be obtained through appropriate scaling of Eq. (1b) [8]. This leads to a powerful analytical expression of the current profile, capable of predicting intricate detail include steep cusp-like rises in the current. An example of which is shown in Fig. 3.

Illustrative Examples

An `elegant` simulation [9] was written to verify a number of illustrative examples showing how control of R_{56} , T_{566} and U_{5666} can allow for a range of final current pulse shapes to be produced. An S-band linac accelerated a bunch off-crest to establish an energy chirp (Fig. 1) that can be described by the 5th order polynomial as,

$$\delta(z_i) \approx 15.8273z_i + 34.1318z_i^2 + 55899.9z_i^3 - 6.449 \times 10^7 z_i^4 + 1.232 \times 10^{10} z_i^5 \quad (2)$$

Equation (2) describes a polynomial fit to the longitudinal phase space distribution before it enters the dispersive region. In the case of these examples, the dispersive region is a dogleg compressor. A lower-order polynomial could be fitted to the distribution data, however in this case a 5th order polynomial was used as it is known that small perturbations in the longitudinal phase space distribution can lead to significant changes to the current pulse shape [8].

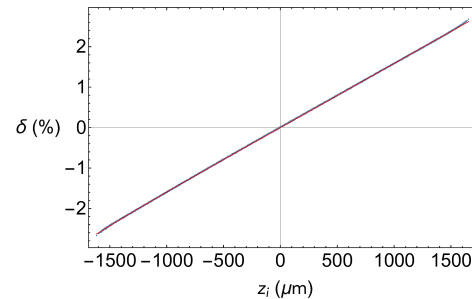


Figure 1: Initial longitudinal phase space distribution used to create the current profiles in Fig. 2. Shown in red is the high order polynomial fit, Eq. (2).

The values of T_{566} and U_{5666} can be varied through altering the strength of sextupole and quadrupole magnets positioned within the compressor. Using `elegant`'s inbuilt optimizer [9], the strength of the sextupole and quadrupole magnets were optimized to reach the desired values of T_{566} and U_{5666} , which are listed in Table 1.

* tessa.charles@monash.edu

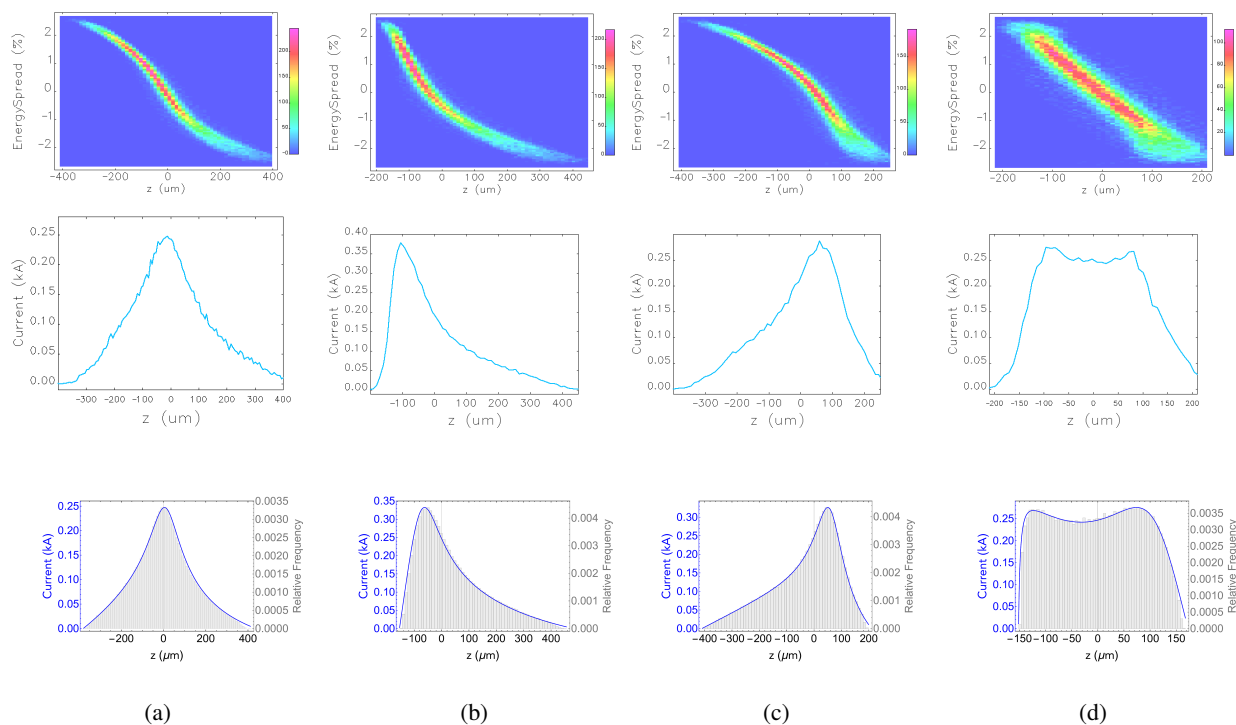


Figure 2: Top row: longitudinal phase space distribution from particle tracking simulations. Middle row: current profile corresponding to the phase space distribution of the top row. Bottom row: current profile given by analytical expression given by Eq. (1). The four columns are the result of propagating a bunch through dispersive regions characterized by different values of R_{56} , T_{566} and U_{5666} , which are summarized in Table 1.

The required values of R_{56} , T_{566} and U_{5666} listed in Table 1, could be achieved through any number of compressor designs that consist of dipoles and sextupoles, with the possible inclusion of quadrupoles and octupoles. In the examples used in this paper, the magnets are arranged in mirror symmetry to ensure that the horizontal dispersion can go to zero at the end of the compressor.

Figure 2 shows the longitudinal phase space and corresponding current profile at the end of the dispersive region for a series of different values of R_{56} , T_{566} and U_{5666} , which are listed in Table 1. The top two rows of Fig. 2 show the elegant simulation results and the bottom row shows the current pulse shape calculated with Eq. (1).

Figure 3 shows additional, more complex examples of pulse shaping. Fig. 3a and Fig. 3b show current profiles that exhibit sharp peaks that are known as caustics. The analytical expression based on Eq. (1) (bottom row) is shown to be capable of accurately describing these sharply rising, cusp-like current pulse shapes. Fig. 3c and Fig. 3d show less typical current pulse shapes to demonstrate the capability of the analytical expression to accurately describe multi-peaked current pulse shapes.

DISCUSSION

The second-order longitudinal dispersion T_{566} , has the effect of shifting current from the head to the tail of the bunch or vice versa. This is evident in Fig. 2b and Fig. 2c where through varying T_{566} , the linear ramp is changed from

Table 1: Longitudinal dispersion values to first-, second- and third-order, required to produce the current pulse shapes in Fig. 2 and Fig. 3.

Current Pulse Shape	R_{56}	T_{566}	U_{5666}
Fig. 2a (triangular)	-70.4 mm	-11.0 mm	-10.0 m
Fig. 2b (ramped left)	-70.4 mm	0.200 m	-3.35 m
Fig. 2c (ramped right)	-70.4 mm	-0.185 m	-5.0 m
Fig. 2d (flat top)	-70.4 mm	-21.0 mm	2.95 m
Fig. 3a	-61.45 mm	-22.0 mm	26.0 m
Fig. 3a	-58.23 mm	-91.5 mm	-6.4 m
Fig. 3c	-58.23 mm	-4.5 mm	-0.8 m
Fig. 3d	-64.0 mm	-2.0 mm	0.25 m

the current pulse sloping from head to tail, to sloping from tail to head.

It is appropriate to question the legitimacy of using the polynomial fit of the initial longitudinal phase space distribution as a sufficient approximation. The similarities between the particle tracking simulations and the analytical expres-

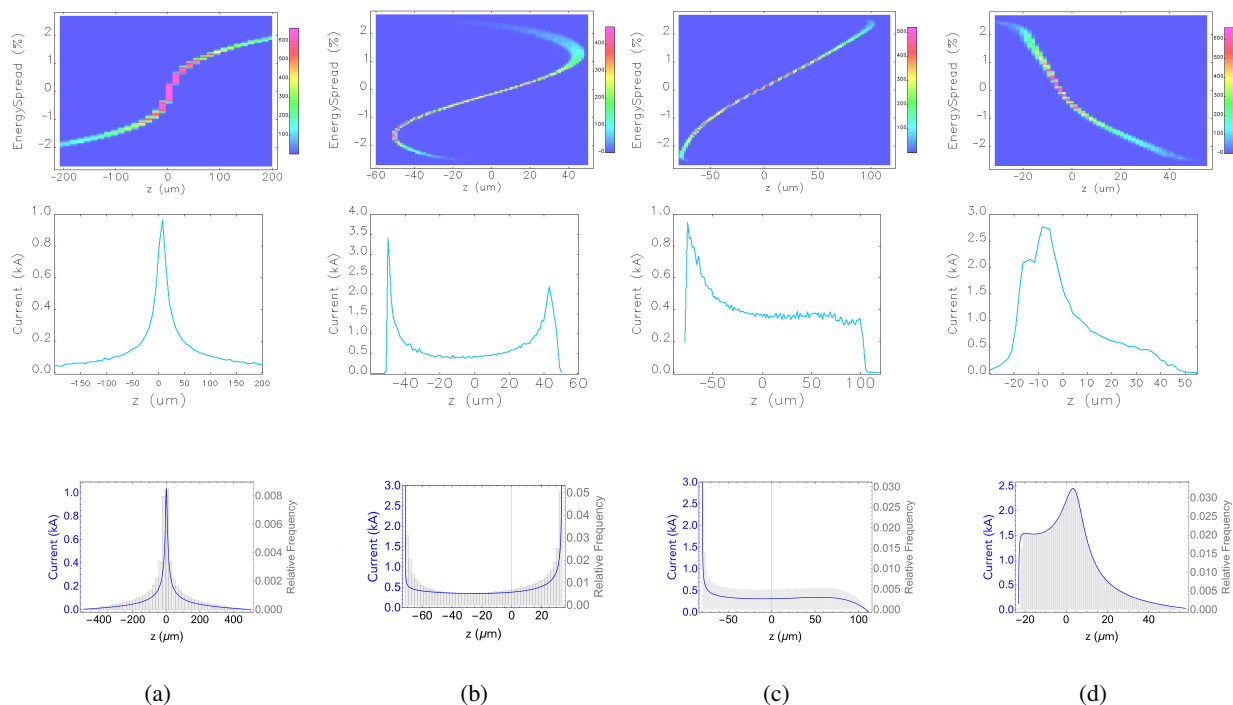


Figure 3: Additional and more complex examples of pulse shaping. Top row: longitudinal phase space distribution from particle tracking simulations. Middle row: current profile corresponding to the phase space distribution of the top row. Bottom row: current profile given by analytical expression. The four columns are the result of propagating a bunch through dispersive regions characterized by different values of R_{56} , T_{566} and U_{5666} , which are summarized in Table 1.

sion (Fig. 2) indicate that in scenarios where an energy chirp is impressed upon the bunch, this polynomial fit provides compelling agreement to the particle tracking results.

Note in the scenarios where caustics are present - identifiable by the sharp rises in the current profile (E.g. Figs. 3a, 3b, and 3c), current pulse shaping is more difficult due to the many-to-one mapping of electron trajectories from initial to final positions in z , making the problem non-invertible. The recent paper by Charles et. al [6] presented a method to eliminate caustics, which forces the mapping of trajectories from initial to final positions to be a one-to-one mapping and therefore invertible.

CONCLUSION

This paper demonstrates how arbitrarily-shaped current pulse shapes can be achieved through ensuring particular values of the first-, second-, and third-order longitudinal dispersion (R_{56} , T_{566} and U_{5666}). Particle tracking simulation results are compared to an analytical expression for the current pulse shape. This analytical expression is capable of describing complex current pulse shapes (including sharply cusp-shaped structures, and multiple peaked structures), and through knowing the analytical form of this expression opens up the possibility tailoring the current pulse shaping for a wide range of accelerator applications.

REFERENCES

- [1] R. J. England, J. B. Rosenzweig, and G. Travish, "Generation and measurement of relativistic electron bunches characterized by a linearly ramped current profile", *Phys. Rev. Lett.*, vol. 100, p. 214802, 2008.
- [2] P. Piot, et al., "Generation and characterization of electron bunches with ramped current profiles in a dual-frequency superconducting linear accelerator", *Phys. Rev. Lett.*, vol. 108, no. 034801, 2012.
- [3] C. Mitchell, J. Qiang, and P. Emma, "Longitudinal pulse shaping for the suppression of coherent synchrotron radiation-induced emittance growth," *Phys. Rev. ST Accel. Beams*, vol. 16, p. 060703, 2013.
- [4] Y. Ding, et al., "Beam shaping to improve the free-electron laser performance at the Linac Coherent Light Source", *Phys. Rev. Accel. Beams*, vol. 19, p. 100703, 2016.
- [5] F. Zhou, K. Bane, Y. Ding, Z. Huang, H. Loos, and T. Raubenheimer, "Measurements and analysis of a high-brightness electron beam collimated in a magnetic bunch compressor", *Phys. Rev. ST Accel. Beams*, vol. 18, p. 050702, 2015.
- [6] T. K. Charles, D. M. Paganin, A. Latina, M. J. Boland, and R. T. Dowd, "Current-horn suppression for reduced coherent-synchrotron-radiation-induced emittance growth in strong bunch compression", *Phys. Rev. Accel. Beams*, vol. 20, p. 030705, 2017.
- [7] M. Cornacchia, S. Di Mitri, G. Penco, and A. A. Zholents, "Formation of electron bunches for harmonic cascade x-ray free electron lasers," *Phys. Rev. ST Accel. Beams*, vol. 9, p. 120701, 2006.

- [8] T. K. Charles, D. M. Paganin, and R. T. Dowd, "Caustic-based approach to understanding bunching dynamics and current spike formation in particle bunches, vol. 19, p. 104402, 2016.
- [9] M. Borland, "Elegant: A flexible SDDS-compliant code for accelerator simulation", *Adv. Phot. Source Report, LS-287*, 2000.